



Unstructured Mesh Finite Element Model for the Computation of Tsunami Scenarios with Inundation

Jörn Behrens
Joern.Behrens@awi.de

Alfred Wegener Institute for Polar and Marine Research,
27570 Bremerhaven, Germany

Summary:

The tsunami simulation software TsunAWI is based on unstructured finite element meshes, utilizing a linear Lagrange conforming and non-conforming finite element numerical discretization method. TsunAWI is used for scenario computations in the German-Indonesian Tsunami Early Warning System (GITEWS) as well as for hazard assessment studies for local disaster management authorities in Indonesia.

The early warning system, developed in the GITEWS framework is introduced under the special focus of the role of simulation. Starting from the non-linear shallow water equations for wave propagation, the discretization method in TsunAWI is described. Some remarks on mesh generation and the inundation scheme follow. The evaluation of an operational model, like TsunAWI, is an important issue and is outlined by examples. Finally some applications like hazard assessment for Padang and inundation mapping for Bali are given.

Keywords:

Tsunami modeling, unstructured mesh, conforming and non-conforming finite elements, inundation map, hazard assessment

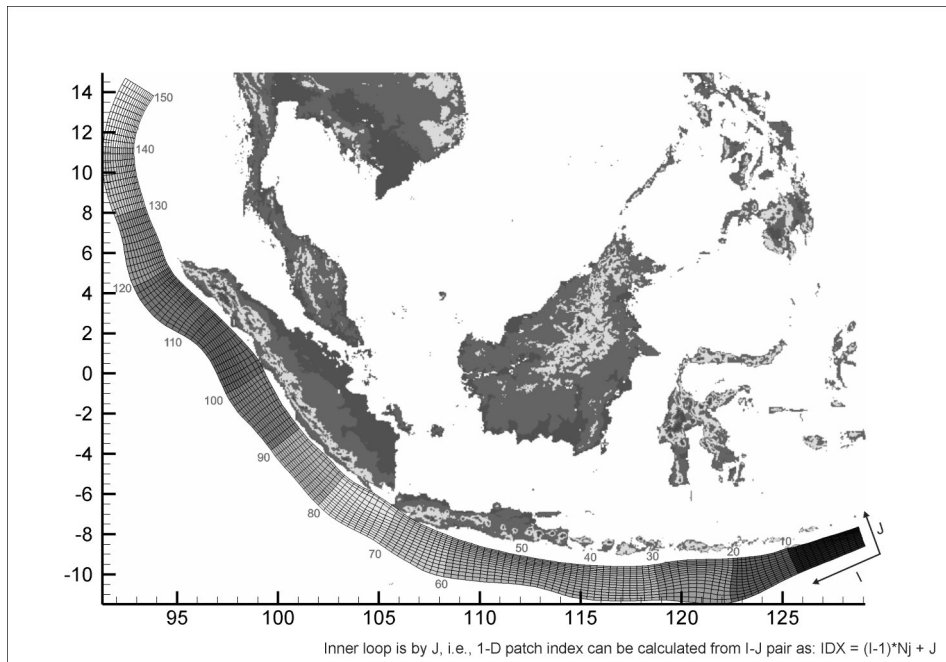


Fig. 1: Grid of patches for the bottom deformation source computation; shading of patches indicates the patch numbering scheme.

1 Introduction

After the devastating tsunami event in the Indian Ocean on December 26, 2004, worldwide activities were triggered to raise awareness and preparedness to such kind of natural hazard. Among the 500 Mio Euro aid funds established by the German Federal Government, some 45 Mio Euro have been dedicated to develop an advanced tsunami early warning system for the Indian Ocean. The German-Indonesian Tsunami Early Warning System (GITEWS), to be installed in Jakarta, Indonesia, is a joint effort of 9 major research institutions in Germany together with partners in Indonesia [7].

At Alfred Wegener Institute (AWI), the author's group is responsible for developing and implementing a simulation system for the GITEWS early warning system. Due to timing constraints, the simulation system will depend on a large number of pre-computed scenarios. In an earthquake event, incoming data from different kinds of sensors are compared to the existing scenarios. In short, the best matching scenario then is selected as the most likely tsunami situation.

The simulation system (SIM) therefore consists of several parts:

- A (large) repository of pre-computed tsunami scenario data;
- A software that generates the tsunami scenarios – we use TsunAWI;
- A selection mechanism;
- A small and quickly accessible data base with scenario values at indexed sensor locations for comparison with incoming sensor measurements;
- A post-processing unit for the generation of warning products.

In this article, the main focus lies on the description of the scenario generating software TsunAWI. But before introducing the background of tsunami modeling, we shall give some basics on the generation of tsunamis in the Indian Ocean.

1.1 Tsunamis in the Indian Ocean

About 90% of the tsunamis in Indonesia are caused by earthquake generated bottom uplift [10]. In the period between 1600 and 1999, more than 100 tsunamis occurred in the region, amounting to a destructive tsunami every four years on average. Approximately 10% of the tsunamis in Indonesia are generated by either volcanic eruptions (9%) or landslides (1%).

While geologists are still debating about the role of the horizontal momentum transfer from the bottom deformation [18], in our simulations we usually assume only vertical bottom deformation as the initial source of tsunami waves. In the current version of the early warning system, only earthquake-generated tsunamis are considered, since the source generation of volcanic and landslide events is much more involved and is still lacking theoretic foundation.

Traditionally, the bottom uplift is modeled by static plate movement (see [12],[13]), the simulations shown in this article use a more sophisticated scheme [1]. We employ 2250 micro-plates (patches) of approx. 45x15 km extension in a grid pattern following the Sunda trench subduction zone along the Indian Ocean Coast of the Indonesian islands of Sumatra, Java, Bali, etc. (see figure 1). These patches are each displaced, using a layered 1D crust model [21]. For larger earthquakes several of these patches are moved with dislocation factors obtained from general scaling laws.

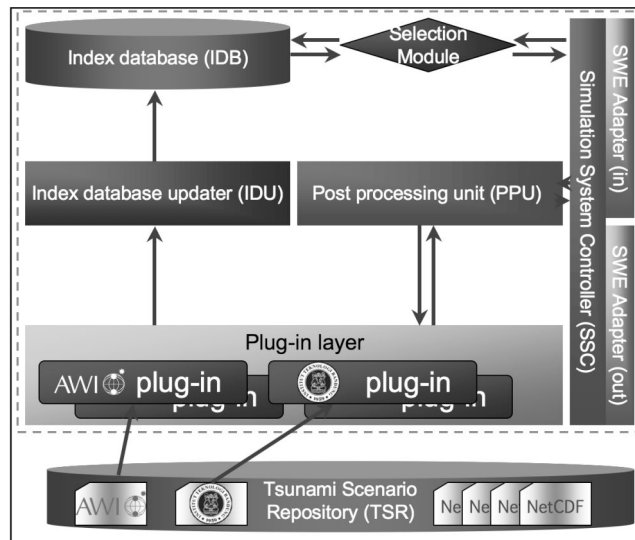


Fig. 2: Internal structure of the GITEWS simulation system.

2 The role of numerical simulation in the GITEWS tsunami early warning system

Unlike most other tsunami early warning systems, which are mainly based on the evaluation of seismic (earthquake) parameters for the generation of early warning situation awareness (see e.g. [6], and [17]), the GITEWS system is based on a simultaneous evaluation of multiple sensor systems. In order to achieve the aim of providing a qualified estimation of the tsunami impact and situation in the near field after only a few minutes, an advanced seismic network and evaluation system SeisComp3 is employed [22]. Additionally, data from wave gauges at coastal positions and in deep ocean (based on buoys), and GPS ground movement sensors are collected in real time.

These measurements are compared to pre-computed tsunami scenario data. The comparison is realized by a weighted 2-norm approach for multiple sensor values. While an online forward computation of the tsunami wave propagation would in principle be possible, it is not advisable to do so. The inversion of the source parameters (i.e. initial conditions) for the tsunami propagation is ill-posed, and therefore highly sensitive to small perturbations in the measurements. A forward computation from these possibly highly perturbed initial conditions would propagate and amplify the error. Therefore, the approach taken here is to compute the whole scenario a priori and compare a consistent set of (possibly perturbed) data with a consistent set of corresponding indexed values from each scenario. The best matching scenario and a number of next best matches are then used for situation awareness and decision support purposes.

The SIM consists of several functional units, depicted in figure 2. The interfaces are realized by Open GIS Consortium (OGC) conforming web service. A controller maintains consistency and takes care for internal workflow. The central logical entity is the selection unit, which implements the multi-sensor comparison. This selection unit works with indexed virtual sensor values from the pre-computed tsunami scenarios, which are stored in a fast and relatively small database – the index database. An index database updater fills the index database from the tsunami scenario's raw data, stored in a tsunami scenario repository. In order to handle diverse types of scenario data and allow for flexible inclusion of third party data, a plug-in layer transparently hides the format details for each individual tsunami scenario away from the SIM. Finally, a post-processing unit generates data products from the scenarios, which can either be accessed after a selection has been performed or preemptively (by scenario ID).

3 Description of the finite element model TsunAWI

The basis for all scenario computations is the unstructured mesh finite-element numerical tsunami simulation software TsunAWI [2].

3.1 Shallow Water Equations

As most current operational tsunami propagation and inundation simulation software systems (see e.g. [9], [20]), we employ the non-linear shallow water equations as the basic set of equations for modeling tsunami wave propagation. These equations are given by

$$\frac{\partial \zeta}{\partial t} + \nabla \cdot (\mathbf{v}H) = 0, \quad (1)$$

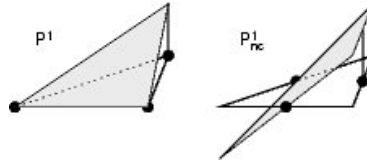


Fig. 3: Conforming P1 (left) and non-conforming P1NC (right) linear Lagrange finite elements.

for the continuity equation, where $H(\mathbf{x},t)=(\zeta(\mathbf{x},t)+h(\mathbf{x}))$ is the total water depth, with ζ the sea surface height (or the deviation from a mean sea surface), h the water depth from bottom to mean sea surface, and $\mathbf{v}(\mathbf{x},t)$ the horizontal velocity vector (\mathbf{x} and t the coordinates in space and time). The momentum equation is given by

$$\frac{\partial \mathbf{v}}{\partial t} + (\mathbf{v} \cdot \nabla) \mathbf{v} + f \times \mathbf{v} + g \nabla \zeta + \frac{C_d \mathbf{v} |\mathbf{v}|}{\rho H} - \nabla \cdot (A_h \nabla \mathbf{v}) = 0, \quad (2)$$

where f is the Coriolis parameter, g is the gravity constant, C_d is a drag coefficient, A_h the horizontal eddy viscosity coefficient. These equations are given in the interior of a bounded domain with time interval $\Omega \setminus \partial\Omega \times [0, T]$, where boundary conditions have to be stated on $\partial\Omega$. Radiation boundary conditions are used at the open lateral boundaries (i.e. open ocean) and either no-slip boundary conditions or inundation boundary conditions at the solid boundaries (i.e. at the coast).

3.2 Finite element discretization

Equations (1) and (2) are discretized, following the lines of Hanert et al. [8]. The special combination of finite elements comprises a conforming P^1 element for representing the functions H , ζ , and h . The velocity-components are represented on a non-conforming P^1_{NC} element, where the unknowns are defined in the edge centers (see fig. 3). This combination of elements has been shown to be stable and free of numerical modes. Denoting by ϕ the basis functions related to the P^1 -element, and \mathbf{w} the basis functions related to the P^1_{NC} -element. Then equations (1) and (2) are expanded in the usual Ritz approach:

$$\int_{\Omega} \left(\frac{\partial \zeta}{\partial t} \phi - H \mathbf{v} \cdot \nabla \phi \right) d\Omega + \int_{\partial\Omega} H \phi \mathbf{v} \cdot \mathbf{n} d\Gamma = 0, \quad \forall \phi. \quad (3)$$

We applied partial integration in order to lift the derivative over to the basis function; \mathbf{n} denotes the outward normal vector. Analogously the momentum equation is expanded:

$$\int_{\Omega} \left(\frac{\partial \mathbf{v}}{\partial t} \cdot \mathbf{w} - (\nabla \cdot (\mathbf{v} \mathbf{w})) \cdot \mathbf{v} + (f \times \mathbf{v}) \cdot \mathbf{w} + g \nabla \zeta \cdot \mathbf{w} + \frac{C_d \mathbf{v} |\mathbf{v}|}{\rho H} \cdot \mathbf{w} - (A_h \nabla \mathbf{v}) \cdot \nabla \mathbf{w} \right) d\Omega + \int_{\partial\Omega} (\mathbf{v} \mathbf{v} \cdot \mathbf{n}) \cdot \mathbf{w} d\Gamma = 0, \quad \forall \mathbf{w}. \quad (4)$$

Again, we have used partial integration to lift derivatives from \mathbf{v} to \mathbf{w} . Additionally, we used arguments as in Hanert et al. to assume

$$\int_{\Omega} (\nabla \cdot A_h \nabla \mathbf{v}) \cdot \mathbf{w} d\Omega \approx \int_{\Omega} (A_h \nabla \mathbf{v} \cdot \nabla \mathbf{w}) d\Omega. \quad (5)$$

In order to derive a computable form of the equations, the usual Galerkin approach is taken for the spatial representation of functions H , ζ , h , and \mathbf{v} in terms of basis function expansions. For example

$$\zeta(\mathbf{x}) \approx \sum_{i=1}^N \zeta_i \phi_i(\mathbf{x}), \quad \mathbf{v}(\mathbf{x}) \approx \sum_{j=1}^M \mathbf{v}_j \mathbf{w}_j(\mathbf{x}),$$

where ζ_i and \mathbf{v}_j are the coefficients while ϕ_i and \mathbf{w}_j are the basis functions corresponding to the i -th vertex and the j -th edge, respectively.

Further on, the domain Ω is triangulated, i.e.

$$\bar{\Omega} = \bigcup_{k=1}^L \bar{\tau}_k, \quad \tau_i \cap \tau_j = \emptyset \quad (i \neq j),$$

where τ_k are the interiors of triangles or elements/cells of the triangulated mesh (see next subsection). These are introduced to construct basis functions with a small support. Due to the non-conforming (i.e. discontinuous) basis functions for velocities, we need to introduce an additional term in order to penalize non-smooth solutions. This term acts on the cell interfaces Γ and is given by

$$\int_{\Gamma} \langle \mathbf{v} \mathbf{v} \cdot \mathbf{n} \rangle_{\lambda} \cdot [\mathbf{w}] d\Gamma, \quad \Gamma = \bar{\tau}_i \cap \bar{\tau}_j, \quad (6)$$

with \mathbf{n} the outward normal vector (related to the cell interface) and

$$\begin{aligned} \langle \nu \rangle_{\lambda} &= \left(\frac{1}{2} + \lambda \right) \nu|_{\tau_i} + \left(\frac{1}{2} - \lambda \right) \nu|_{\tau_j}, \quad \lambda \in \left[-\frac{1}{2}, \frac{1}{2} \right], \\ [\nu] &= \nu|_{\tau_i} - \nu|_{\tau_j}, \end{aligned}$$

the jump and the weighted average, resp. Omitting the time dependence for the moment, we derive the discretized equations (using some further algebra and simplifications as outlined in [8]). The continuity equation then reads

$$\sum_{k=1}^L \int_{\tau_k} \left(\frac{\partial \zeta^h}{\partial t} \phi_l - H^h \mathbf{v}^h \cdot \nabla \phi_l \right) d\Omega + \sum_{j=1}^M \int_{\Gamma_j} \left(\sqrt{gH} \zeta^h \phi_l \right) d\Gamma = 0, \quad l = 1 : N \quad (7)$$

while the discrete momentum equation is given by

$$\begin{aligned} \sum_{k=1}^L \int_{\tau_k} \left(\frac{\partial \mathbf{v}}{\partial t} \cdot \mathbf{w}_j - \mathbf{v}^h \nabla \cdot (\mathbf{v}^h \mathbf{w}_j) + (f \times \mathbf{v})^h \mathbf{w}_j + g \nabla \zeta^h \mathbf{w}_j + \frac{C_d \mathbf{v}^h |\mathbf{v}^h|}{\rho H^h} \mathbf{w}_j - A_h \nabla \mathbf{v}^h \right) \cdot \nabla \mathbf{w}_j d\Omega + \\ + \sum_{j=1}^M \int_{\Gamma_j} \langle \mathbf{v}^h \mathbf{v}^h \cdot \mathbf{n} \rangle_{\lambda} [\mathbf{w}_j] d\Gamma = 0, \quad j = 1 : M. \end{aligned} \quad (8)$$

We have used the index $k=1:L$ for the L elements τ_k of the mesh, $j=1:M$ for the M interior cell interfaces (edges) Γ_j , $l=1:N$ for the N vertices, and the superscript h indicates that we use the Galerkin-expansion of the corresponding functions.

The time derivative is treated by an explicit centered time difference (leap-frog scheme), as used for example in [9]. In order to achieve numerical efficiency, we apply mass lumping for the arising system of equations, which gives explicit formulas for the prognostic variables \mathbf{v}^h and ζ^h .

3.3 Unstructured mesh

In the previous section, the numerical scheme for solving shallow water wave propagation equations was derived. However, a crucial part in each simulation is the mesh generation, since the topographic features in the ocean demand for adequate triangulations. Since the numerical scheme uses explicit time stepping, strong stability constraints – in particular the Courant-Friedrichs-Levy condition (CFL) – have to be respected. This condition demands the time step Δt and/or the mesh size $\Delta \mathbf{x}$ to be adjusted to guarantee that the Courant number C does not exceed 1 for the phase speed \mathbf{V} :

$$C = \mathbf{V} \frac{\Delta t}{\Delta \mathbf{x}} < 1.$$

Fortunately, the physical properties of wave propagation phenomena help in fulfilling both constraints, an adequately highly resolved mesh for appropriate coastline representation and stability.

Wave speed in linear theory is proportional to the water depth, since the following relation holds

$$\mathbf{V} \approx \sqrt{gH}.$$

The Courant number will be uniform, if the mesh size is chosen proportional to water depth. Additionally, rapidly changing topography is to be well resolved. Therefore, a resulting criterion for the cell size $\Delta \mathbf{x}$ is given by (c_t and c_g two adjustable constants):

$$\Delta \mathbf{x} \leq \min \left\{ c_t \sqrt{gH}, c_g \frac{h}{\nabla h} \right\}. \quad (9)$$

The grid generation process starts from given bathymetric (i.e. the topography below sea level) and topographic data. Usually a digital terrain or elevation model (DTM or DEM, resp.) is given. In our case, the bathymetry is generally given by GEBCO data [19], and topography data are taken from SRTM shuttle radar mission [16]. Some more data have to be given:

- A coast line is defined by a polygon,
- An open ocean boundary of the domain of interest is defined,
- An upper terrain/maximum inundation line inland is defined. In our meshes, this is either a 50m-elevation iso-line or a 7 km coastal distance line [4].

With these input data, an automatic Delaunay triangulation software (triangle by J.R. Shewchuk [14]) is utilized to triangulate the computational domain. Finally several grid smoothing techniques are applied to further enhance the grid quality. A detail of one of our typical meshes is depicted in figure 4.

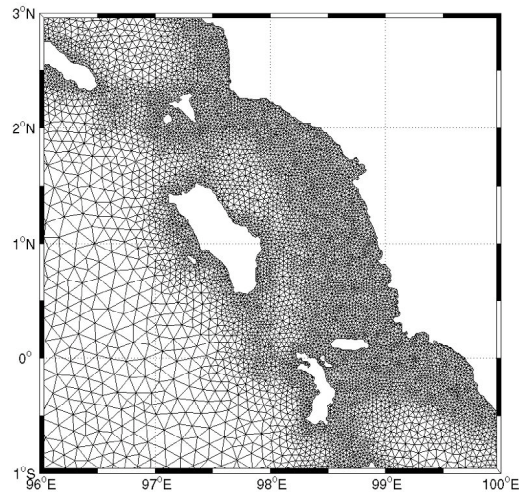


Fig. 4: Typical mesh for tsunami wave propagation computations; the area shows Nias Island to the West of Sumatra/Indonesia.

3.4 Inundation scheme

The inundation boundary condition follows the ideas of Lynett et al [11]. In general, the idea behind this inundation scheme is to define cells to be either wet or dry or partly dry. In the explicit solution scheme, the momentum equation is solved, using height values from the previous time step on the right hand side, while the continuity equation uses just computed velocity values. For the pressure gradient term, the inundation has to be extrapolated in the momentum equation. In principle, the momentum needs also to be extrapolated for the continuity equation, but for simplicity and risking a slightly dissipative behavior of the run-up scheme, we omit this step.

Therefore, only in the continuity equation computation, an extrapolation of values of ζ is performed. Two different extrapolation schemes are employed:

- A linear extrapolation based on the finite element representation of ζ ,
- A linear least squares approximation based on neighboring wet unknowns, which is slightly better behaved, with respect to smooth solutions and non-linear equations.

This inundation scheme has been evaluated by an analytical test case, as well as real life field data, as shown in the next chapter.

4 Validation of TsunAWI

Operational tsunami simulation software needs to be validated and tested. Besides of usual software correctness tests, a suite of increasingly complex functionality tests is performed. These tests have been agreed within the international tsunami modeling community. Simple tests comprise the recording of mass conservation, which is exactly maintained by TsunAWI, due to the discretization scheme (flux form continuity equation with corresponding structure preserving finite element discretization). Analytical test cases in quasi one-dimensional settings form the next complexity level. One such example tests the capability of an inundation scheme to represent the receding and inundating wave behavior. The result is shown in figure 5.

Some measurements from laboratory experiments are available and currently used for validation of tsunami models. The final stage of complexity is represented by real life tsunami event field data, which the simulation is required to reproduce. The Boxing Day Tsunami of 2004 (Great Andaman-Sumatra tsunami) tragically provided very valuable field data for model evaluation [23]. Other tsunamis are the Hokkaido Nansei-Oki Tsunami of 1993 [15], and the 17 Juli 2006 Java Tsunami [5], among others. Additionally, the simulation results of different models can be compared in model intercomparison studies.

All these tests have been performed with TsunAWI. A comprehensive documentation of this evaluation and an automatic testing procedure for new model versions is in preparation, and will be available in the near future.

5 Examples of TsunAWI's application

One of the most important simulation results of a tsunami wave propagation model in the framework of an early warning system is to provide arrival time information. While for preliminary hazard assessment arrival time computations based on linear theory and with one-dimensional ray-tracing-type simulation tools appears to be efficient and sufficient, in the case of complex coastline and near-field earthquake situations like in Sumatra, this approach is not suitable. Therefore, visualization of the

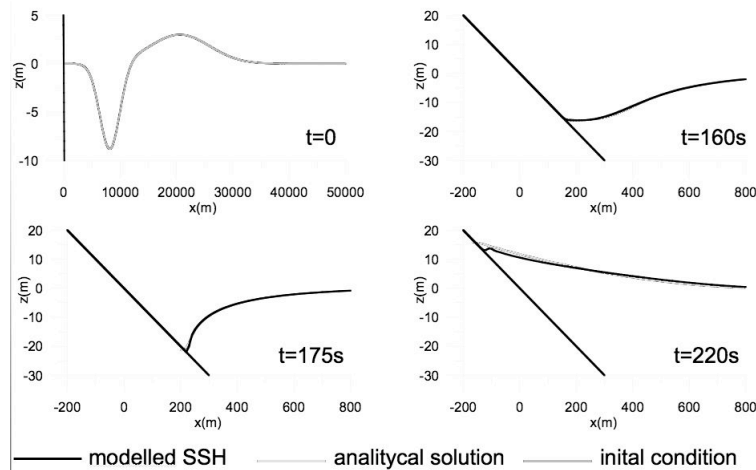


Fig. 5: Results of analytical test case for inundation modeling. Wave recession and run-up corresponds well with the analytical solution.

isochrones of first wave arrival is a very effective way to assess the situation and give guidance in the warning process to local authorities.

Arrival time information is also important for preparedness planning efforts. Disaster managers need to know the timing constraints for the planned activities. Evacuation measures take time, so arrival times are crucial information.

For preemptive hazard and risk assessment, other values may be of interest. In the tsunami scenarios, provided by TsunAWI, the following values are stored and can be used in post-processing:

- Time of first arrival of a water elevation of more than 0.01 m;
- Sea surface height (SSH or flow depth on land, ζ) every 60 seconds as a snapshot;
- Maximum SSH;
- Maximum absolute value of velocity;
- Maximum flux density (for impact assessment);
- Initial bottom uplift.

All of the above listed values are given on mesh vertices. The scenario raw data are stored in NetCDF file format, which provides a machine independent and self-describing binary data format. The SIM's post processing unit derives different types of ESRI shape files from these for visualization and analysis purposes in a GIS environment.

In general TsunAWI is used for two main purposes:

1. To generate a set of scenarios for the SIM tsunami scenario repository,
2. To generate scenarios for hazard assessment and inundation studies.

In this section, we show examples of both these applications.

5.1 Scenario computations and sensitivity analysis

A large number of pre-computed scenarios will serve as a basis of possible expected situations in the SIM's repository. Each of these scenarios represents one possible location and magnitude of an earthquake with corresponding dislocations at GPS sensor positions and bottom uplift. In the near field the exact source (initial condition) is extremely important for exact hazard assessment. We may – for example – look at Padang, the capital of the province of West-Sumatra with a population of a little less than a million. Corresponding to current geophysical knowledge this city is threatened by a major rupture due to an inter-plate locking situation [3]. In order to assess the sensitivity on the location of the rupture, a number of scenarios can be utilized to see that very close (but different) earthquake locations may lead to completely different inundation results. The special situation of Padang with the Mentawai Islands shielding away tsunami wave energy from open ocean tsunami events, but trapping tsunami wave energy from near shore events, yields a very large sensitivity on the exact location of the rupture (figure 6).

5.2 Inundation modeling for Bali

One of Indonesia's famous tourist areas is located on Bali. Many resorts and hotels have been built directly at the shore. The larger Denpasar area, featuring an international airport with 1.5 Mio check-ins per year, has a population count of approx. 500,000. Most of its territory lies below 25 m above sea level and is vulnerable to tsunami inundation. In order to provide planning tools for future tsunami preparedness, inundation simulations have been performed for the Denpasar region.

Accurate topography and bathymetry data, especially for near-shore areas, is necessary to obtain realistic results. The mesh used in these computations has a cell size of approx. 80 m near shore and

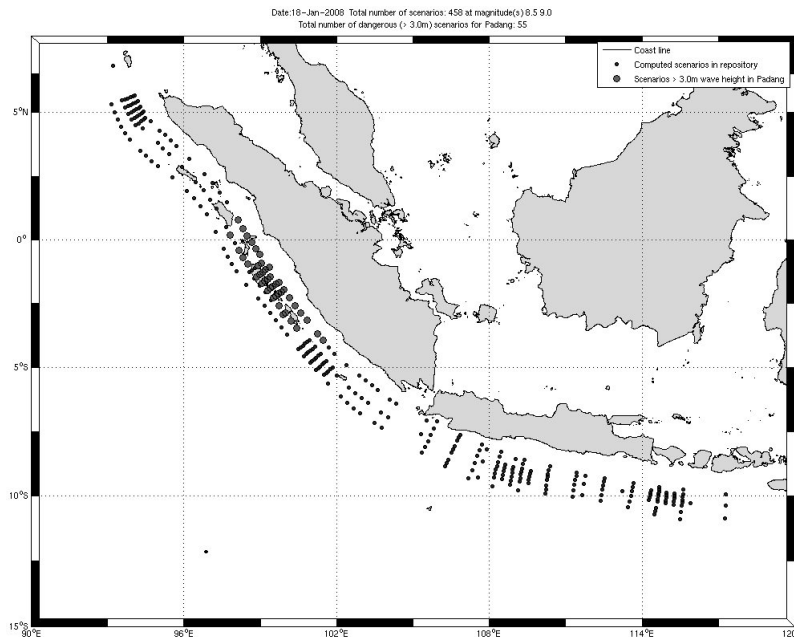


Fig. 6: Locations of scenarios of earthquake moment magnitude 8.5 and 9 along the Indian Ocean coast; among all scenarios only the bold ones yield wave heights > 3 m at the shore in Padang.

on land in Denpasar. The worst case inundation map shown in figure 7, projects devastating flow depths of above 5 m, corresponding to a magnitude 8.5 earthquake approx. 150 km to the South-West, to the populated region close to Denpasar. It is noticeable that the airport encounters particularly high water levels, which has to be taken into account for future evacuation and aid support planning measures. Inundation lines of more than 3 km from the shoreline also indicate that horizontal evacuation measures might not be sufficient, but have to be complemented by vertical evacuation.

6 Conclusions

In this article, we introduced the new unstructured mesh finite element tsunami wave propagation and inundation simulation tool TsunAWI. It is based on non-linear shallow water theory and includes Coriolis, bottom friction and viscosity forcing terms. The discretization scheme is based on linear Lagrange finite elements, which are conforming for the sea surface height disturbance (scalar functions) and non-conforming for the velocities.

Advanced semi-automatic mesh generation allows for very accurate local resolution along the shore and in regions of interest, while maintaining coarse resolution (and hence efficiency) in deep ocean. This seamless and smooth transition from large to small grid size does not lead to numerical artifacts like spurious wave reflections.

TsunAWI has been evaluated, using analytical test cases as well as model inter-comparison studies and real-life field measurement based test cases. It proves to be very accurate and useful for inundation studies, sensitivity analysis, and hazard assessment. Tsunami scenarios generated with this tool will be used in the simulation system of the GITEWS tsunami early warning system, to be installed in Jakarta/Indonesia in November 2008.

Future activities will include a major code revision to keep up with state of the art software development standards and to allow easy maintenance. Parallelization will be another important feature, necessary for conducting even larger simulations in shorter time and to eventually achieve a real-time capability of the forward simulation. Further evaluation and testing is also planned to further stabilize the reliability of the simulation results.

The source code of TsunAWI will be available under a GPL-like open source license, allowing scientists and engineers from tsunami-prone regions to perform their own detailed simulations.

7 Acknowledgements

The author would like to acknowledge the contributions of Alexey Androsov, Lars Mentrup, Florian Klaschka, Sven Harig, Widodo Pranowo, and Haiyang Cui, all members of the Tsunami Modeling Group at AWI. Some of the figures were created, using tools for Google Earth kml-file creation by Pascal Schmitt. Parts of the implementation of TsunAWI originate from Dmitry Sein and Dmitry Sidorenko. Figure 1 is reproduced with permission of A. Babeyko.



Fig. 7: Inundation map for Denpasar area, Bali/Indonesia.

8 References

- [1] Babeyko, A. Y. and Sobolev, S. V.: "Modeling Stress in the Subducting Slab With Complex Elasto-Visco-Plastic Rheology", EOS Trans. AGU, 2006, Vol. 87, Abstract T13C-0521.
- [2] Behrens, J., Androsov, A., Braune, S., Danilov, S., Harig, S., Schröter, J., Sein, D. V., Sidorenko, D., Startseva, O., Taguchi, E.: "TsunAWI Technical Documentation Part I: Mathematical, numerical and implementation concepts", Tsunami Project Documentation No. 004, 2007, Bremerhaven, Germany.
- [3] Borrero, J. C., Sieh, K., Chlieh, M., and Synolakis, C. E.: "Tsunami inundation modeling for western Sumatra", PNAS, 2006, Vol. 103, pp. 19673–19677.
- [4] Braune, S., Harig, S., Behrens, J., Schröter, J., and Hiller, W.: "Erzeugung eines geeigneten Finite-Elemente-Gitters für Tsunami-Simulationsrechnungen aus mehreren Datenquellen", in Angewandte Geoinformatik 2007. Beiträge zum 19. AGIT-Symposium Salzburg (Strobl, J. and Blaschke, T. and Griesebner, G.), Herbert Wichmann Verlag, Heidelberg, 2007, pp. 85–90.
- [5] Fritz, H. M., Kongko, W., Moore, A., McAdoo, B., Goff, J., Harbitz, C., Uslu, B., Kalligeris, N., Suteja, D., Kalsum, K., Titov, V., Gusman, A., Latief, H., Santoso, E., Sujono, S., Djulkarnaen, D., Sunedar, H., and Synolakis, C. E.: "Extreme runup from the 17 July 2006 Java tsunami", Geophysical Research Letters, 2007, Vol. 34, p. L12602 ff.
- [6] Furumoto, A. S. and Tatehata, H. and Morioko, C.: "Japanese Tsunami Warning System", Science of Tsunami Hazards, 1999, Vol. 17, pp. 85–105.
- [7] GITEWS Homepage: <http://www.gitews.de>.
- [8] Hanert, E., Le Roux, D. Y., Legat, V., and Deleersnijder, E.: "An efficient Eulerian finite element method for the shallow water equations", Ocean Modelling, 2005, Vol. 10, pp. 115–136.
- [9] Imamura, F., Yalciner, A. C., Ozyurt, G.: "Tsunami Modelling Manual", 2006.
- [10] Latief, H., Puspito, H. T., and Imamura, F.: "Tsunami Catalog and Zones in Indonesia", Journal of Natural Disaster Science, 2000, Vol. 22, pp. 25–43.
- [11] Lynett, P. J., Wu, T.-R. and Liu, P. L.-F.: "Modeling wave runup with depth-integrated equations", Coastal Engineering, 2002, Vol. 46, pp. 89–107.
- [12] Mansinha, L. and Smylie, D. E.: "The displacement fields of inclined faults", Bulletin of the Seismological Society of America, 1971, Vol. 61, pp. 1433–1440.
- [13] Okada, Y.: "Surface deformation due to shear and tensile faults in a half-space", Bulletin of the Seismological Society of America, 1985, Vol. 75, pp. 1135–1154.

- [14] Shewchuk, J. R.: "Triangle: Engineering a 2D Quality Mesh Generator and Delaunay Triangulator", in *Applied Computational Geometry: Towards Geometric Engineering* (Lin, M. C. and Manocha, D.), Springer Verlag, 1996, Vol. 1148, pp. 203–222.
- [15] Shuto, N. and Matsutomi, H.: "Field Survey of the 1993 Hokkaido Nansei-Oki Earthquake Tsunami", *PAGEOPH*, 1995, Vol. 144, pp. 649–663.
- [16] Shuttle Radar Topography Mission (SRTM): <http://www.dlr.de/srtm/>.
- [17] Sokolowski, T. J.: "The U.S. West Coast and Alaska Tsunami Warning Center", *Science of Tsunami Hazards*, 1999, Vol. 17, pp. 49–55.
- [18] Song, Y. T., Fu, L.-L., Zlotnicki, V., Ji, C., Hjorleifsdottir, V., Shum, C. K., and Yi, Y.: "The role of horizontal impulses of the faulting continental slope in generating the 26 December 2004 tsunami", *Ocean Modelling*, 2008, Vol. 20, pp. 362–379.
- [19] The General Bathymetric Chart of the Oceans (GEBCO): "GEBCO 1-minute global bathymetric grid", <http://www.ngdc.noaa.gov/mgg/gebco/grid/1mingrid.html>.
- [20] Titov, V. and Gonzalez, F. J.: "Implementation and Testing of the Method of Splitting Tsunami (MOST) Model", NOAA Technical Memorandum ERL PMEL-112, 1997, Seattle, WA, USA.
- [21] Wang, R., Martin, F. L., and Roth, F.: "Computation of deformation induced by earthquakes in a multi-layered elastic crust—FORTRAN programs EDGRN/EDCMP", *Computers & Geosciences*, 2003, Vol. 29, pp. 195–207.
- [22] Weber, B., Becker, J., Hanka, W., Heinloo, A., Hoffmann, M., Kraft, T., Pahlke, D., Reinhardt, J., Saul, J., and Thoms, H.: "SeisComP3 - automatic and interactive real time data processing", *Geophysical Research Abstracts*, 2007, Vol. 9, p. 09219.
- [23] Wijetunge, J. J.: "Tsunami on 26 December 2004: Spatial Distribution of Tsunami Height and the Extent of Inundation in Sri Lanka", *Science of Tsunami Hazards*, 2006, Vol. 24, pp. 225–239.